International Journal of Engineering Trends and Technology
ISSN: 2231-5381/ https://doi.org/10.14445/22315381/IJETT-V73I3P141

Volume 73 Issue 3, 581-589, March 2025

Original Article

Grid Interconnection of Renewable Sources with Three-phase Transformer-Less Boost Multilevel Inverter Topology with Reduced Harmonics

Gaddam Bhagyalaxmi[1], Balasubbareddy Mallala[2], P. Satish Kumar[3]

[1,3] *University College of Engineering (Autonomous), Osmania University, Hyderabad, Telangana, India.*
[2] *Chaitanya Bharathi Institute of Technology, Hyderabad, Telangana State, India.*

[1]*Corresponding Author : gblaxmi5063gaddam@gmail.com*

Received: 9 December 2024 Revised: 11 February 2025 Accepted: 4 March 2025 Published: 28 March 2025

Abstract *- Connecting renewable sources in parallel to the grid with conventional sources is a challenging task. As the output of renewable sources is unstable, it needs to be stabilized using several passive and active elements to share power with the grid. The circuit system needs to be more efficient and stable with reduced ripple and harmonic content. In this paper, a three-phase transformer-less boost MLI topology is introduced with a PV array and PMSG wind farm renewable sources connected to the input. The MLI is connected to the grid through an LC passive filter to mitigate harmonic content. The proposed MLI has voltage-dividing capacitors to create voltage levels. The inverter comprises two stages, which include a voltage-level generator circuit and an inverting circuit. The voltage level generator circuit creates multilevel voltages only in a positive direction. The multilevel DC voltage is converted to AC by the inverting circuit, sharing power with the grid. The reference signal to the multilevel inverter pulse modulation technique controller is generated by modified fuzzy MPPT-based p-q control theory for efficient renewable power sharing to the grid. The boost converter at the input of the multilevel inverter ensures maximum power extraction controlled by the MPPT technique. The multilevel inverter ensures reduced harmonic AC voltage generation for sharing PV array power with low THD value to the grid.*

Keywords *- Multi-Level Inverter (MLI), Photo Voltaic (PV), Permanent Magnet Synchronous Generator (PMSG), L-C-L (Inductor-Capacitor-Inductor), Active and reactive power (p-q), Maximum Power Point Tracking (MPPT), Total Harmonic Distortion (THD).*

1. Introduction

In order to reduce the environmental temperatures due to global warming, conventional fossil fuel power generation needs to be replaced with zero-emission renewable sources [1]. Renewable energy sources, such as solar, wind, hydro, and geothermal, produce little to no carbon dioxide, which helps in the fight against climate change. Unlike fossil fuels, renewable energy reduces pollutants like Sulphur dioxide, nitrogen oxides, and particulate matter, improving air and water quality [2]. These sources harness natural processes-like sunlight and wind-rather than relying on finite resources like coal or oil. However, large-scale renewable projects, such as hydroelectric dams and wind farms, can disrupt local ecosystems and harm wildlife [3]. PV array and PMSG wind farm renewable sources are considered more reliable and flexible for installation from the many available renewable sources. The capital cost for integrating PV arrays and wind farms is also very low compared to biogas plants, fuel cell units, etc [4]. The PV array has multiple solar panels connected in series and parallel array combinations for generating power absorbing sunlight [5]. However, utilizing the power from the PV array is difficult as the current generated is DC, and the power is unstable due to unreliable solar radiation. The PV array must be connected to power and voltage stabilizing circuits with an inverting operation to connect to the conventional grid.

The PMSG wind farm is integrated with a rectifier and DC/DC converter for voltage stabilization. In traditional topology, the PV array and PMSG wind farm are connected to a simple boost converter operated by the MPPT technique, extracting maximum power from the panels and PMSG with boosting voltage. Later, the boosted DC voltage is inverted using a PWM inverter to generate AC voltage [6]. The conventional PWM inverter has heavy harmonic content, which is mitigated using high-rating LC filters. This increases the complete setup's size, volume and cost, reducing efficiency and reliability. In order to reduce the sizing of the harmonic filter, the conventional inverter is replaced with transformer-less boost MLI.

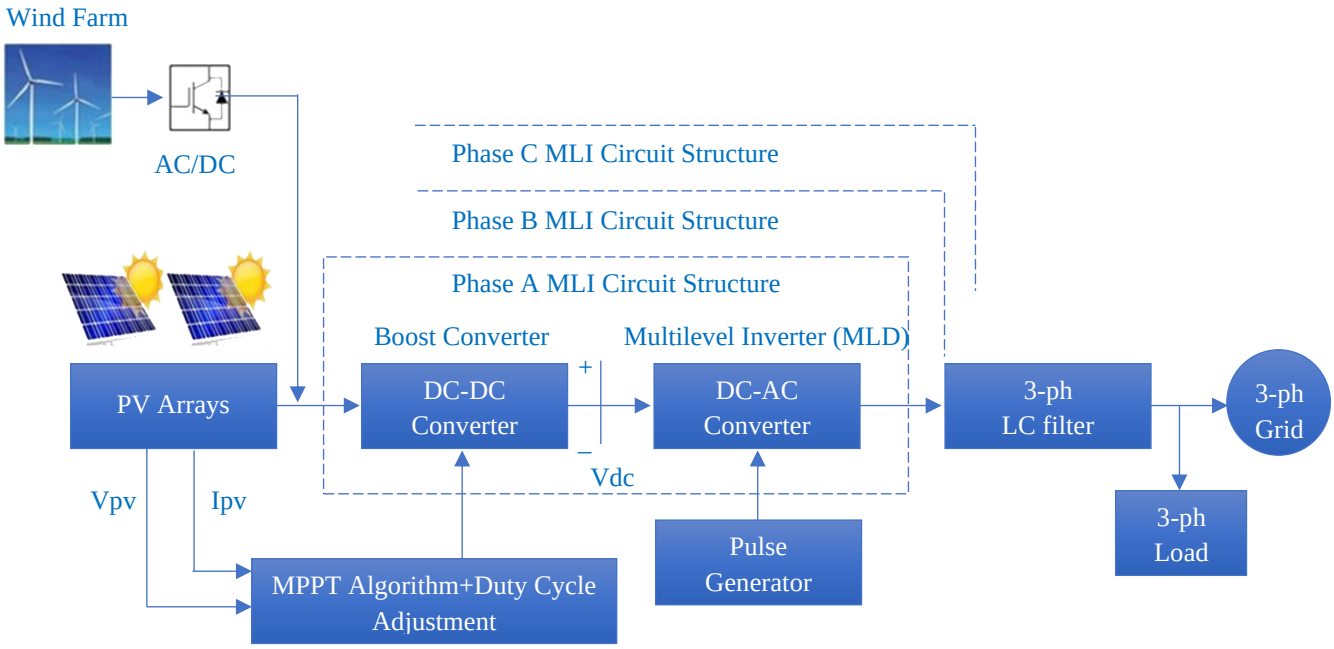

Fig. 1 Outline the structure of the proposed circuit topology

The proposed MLI generates multilevel voltages in the positive and negative directions, replicating a sinusoidal voltage [7]. The outline of the three-phase grid interconnection of the PV array and PMSG wind farm with three-phase transformer-less boost multilevel inverter topology is presented in Figure 1. As presented in Figure 1, the PV array and wind farm are connected to a DC-DC converter operated with an MPPT algorithm and duty cycle adjustment controller. This controller takes feedback from the PV array voltage and current (Vpv and Ipv) using the signals to generate a reference duty ratio for the converter [8]. The DC voltage from the PV array and wind farm is boosted and stabilized by the boost converter fed to the MLI [9]. The three-phase MLI then converts the boosted DC voltage to multilevel AC voltage connected to the grid through an LC filter. As observed, this topology prevents the transformer from stepping up the voltage, reducing the cost and power loss of the system. The MLI is controlled by a pulse generator with respect to the grid voltage phase and frequency [10]. The reference signals to the MLI are produced by the modified fuzzy-based p-q control theory, which has a PLL (Phase Locked Loop) module for grid synchronization. The paper is organized with an introduction to the proposed system and its outline structure in section 1, followed by the design of the proposed MLI topology in section 2. Section 2 includes the pulse patterns of the switches and the operating modes of the MLI. Section 3 presents the modified fuzzy-based p-q control theory structure with mathematical expressions. The control for generating the reference signal for the MLI is presented in Section 3. The simulation results for the proposed system with different operating conditions set in the model are presented in Section 4. The generated graphs of all the modules are analysed by finalizing the results and validating the system in Section 5. The references cited in this paper are given after Section 5.

2. Proposed MLI Topology

There are several conventional Multilevel Inverter (MLI) topologies, such as cascaded H-bridge, diode clamp, and clamping capacitor, which generate multilevel Pulse Width Modulation (PWM) voltages. These multilevel PWM voltages exhibit very low harmonic content when operating at high frequencies [11]. However, the increased number of switches required in these MLIs leads to higher power losses, negatively impacting system efficiency. In diode-clamped and flying capacitor MLIs, balancing the voltage across capacitors or diodes becomes complex, especially at higher voltage levels. Additionally, managing the heat produced by numerous components can be challenging, particularly in high-power applications. The necessity for a large number of high-quality components also raises initial investment costs. Furthermore, the space and cost demands for incorporating additional levels can limit scalability. These MLIs must be replaced with reduced switches and advanced control techniques for reduced power loss, high efficiency and low THD inverters. The next-generation MLIs have a low number of switches, but the input sources needed are more than one. One of the most used advanced inverters is the switched capacitor MLI, which has multiple voltage-dividing capacitors for creating multilevel voltages [12]. As the number of input sources is to be more than one, the switched capacitor MLI cannot be used for a single source like a PV array, battery or

fuel cell. These MLIs operate at very high frequencies to generate PWM voltages, resulting in high input current ripples. These high current ripples are a drawback for achieving maximum power extraction from renewable sources. Managing the switching sequences for multiple levels is challenging, requiring sophisticated algorithms. These MLIs may not be suitable for certain load conditions or applications, such as those requiring extremely fast dynamic response [13]. Asymmetrical input source voltage requirement creates another challenge for these inverters. A novel transformer-less boost multilevel inverter topology is proposed to overcome the aforementioned power quality issues of the conventional MLI. The circuit structure of the proposed MLI can be observed in Figure 2.

In the presented circuit structure Figure 2, at the input, a PV array and PMSG wind farm are connected as sources with a boost converter connected for voltage gain. The maximum power from the PV array is delivered to the inverter by controlling the Q_b MOSFET switch by the MPPT algorithm [14]. The L_{in} is the boosting inductor for storing charge and creating voltage gain at the output given as

$$L_{in} \geq \frac{V_{in}D}{f_s \Delta I_{Lin}} \quad (1)$$

Here, Vin is the input voltage, D is the duty ratio of the switch Qb, f_s is the switching frequency of the Qb, ΔI_{Lin} is the allowable current ripple percentage of inductor L_{in}. The number of levels in the MLI is considered with respect to the number of switches connected in the voltage level generation circuit, which is given as

$$N = 2n + 1 \quad (2)$$

Here, N is the number of levels, and n is the number of switches. Number of diodes and capacitors is given as

$$N_{diode} = N_{cap} = N - 2 \quad (3)$$

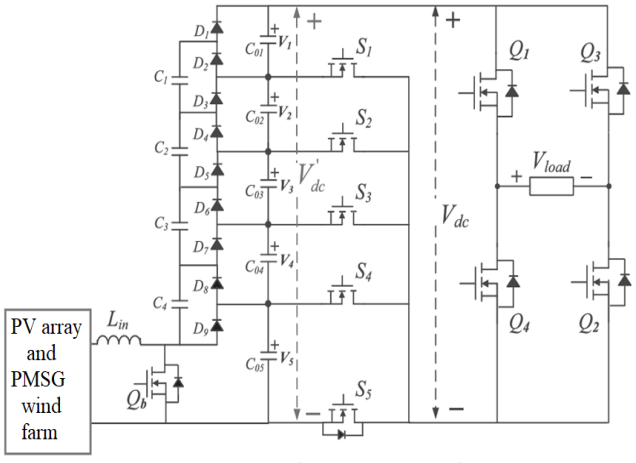

Fig. 2 Circuit structure of proposed MLI of one phase

In the next stage, a voltage dividing and clamping circuit with multiple capacitors and diodes is connected [15]. The capacitors (C_1-C_4) are considered to be clamping capacitors, diodes (D_1-D_9) are freewheeling diodes, and capacitors (C_{01} – C_{05}) are the voltage-dividing capacitors. The value of the capacitors is calculated as

$$C_i \geq \frac{I_{out}D}{f_s \Delta V_{Ci}} \quad (4)$$

Here, I_{out} is the output current of the inverter and ΔV_{Ci} is the allowable voltage ripple percentage of capacitor C_i. MOSFET switches (S1-S5) are used to create multiple voltage levels with a body diode connected to only the S5 switch. The switching pattern and the switching cycle of the multilevel voltage generator are presented in Figure 3 and Table 1. As Figure 3 and Table 1 observed, the voltage levels are created by switching off the MOSFET switches (S1-S5) at different time intervals with a phase delay.

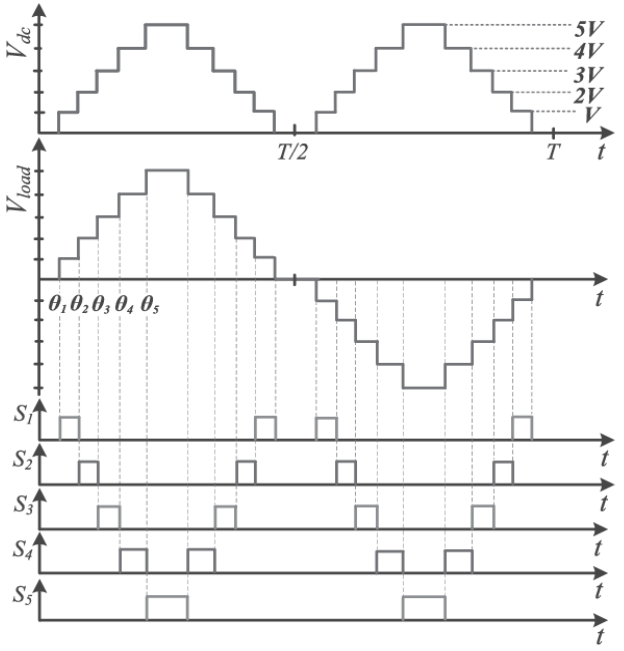

Fig. 3 Switching pattern of the MLI MOSFET switches (S_1-S_5)

Table 1. Switching cycle

State	ON switches	Output voltage
1	All OFF	0V
2	S1 Q1 Q2	+V
3	S2 Q1 Q2	+2V
4	S3 Q1 Q2	+3V
5	S4 Q1 Q2	+4V
6	S5 Q1 Q2	+5V
7	S1 Q3 Q4	-V
8	S2 Q3 Q4	-2V
9	S3 Q3 Q4	-3V
10	S4 Q3 Q4	-4V
11	S5 Q3 Q4	-5V

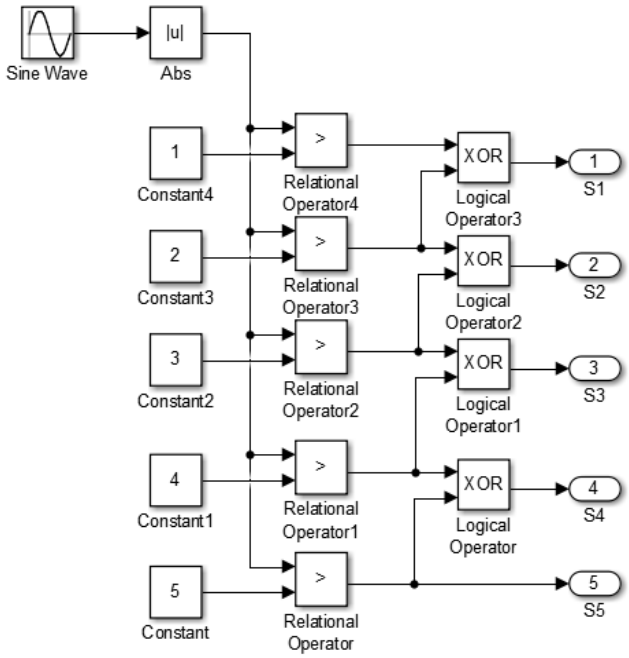

Fig. 4 Logic controller for multilevel voltage switches

The positive and negative AC voltages are created by the Q1-Q4 switches, which are the inverting circuit [16]. For positive multilevel voltage generation, Q1 and Q2 are turned ON, and for negative multilevel voltage generation, Q3 and Q4 are turned ON. The pules to the switches are generated by a Sinusoidal reference voltage signal compared to voltage levels. The Logic controller for generating the pulses for the switches (S1-S5) is presented in Figure 4. As per the reference signal (Sin Wave) input to the Logic controller the switches operate with phase delay created as per the shape of the Sinusoidal waveform. The output of the MLI tends to replicate the reference signal given to the controller. For the proposed grid-connected system, the reference signal is generated by a modified p-q controller with grid voltage synchronization discussed in Section 3.

3. Controller Design

As mentioned in previous sections, the reference signal for controlling the three-phase inverter of the PV array and wind farm-connected MLI is generated by a modified fuzzy-based p-q controller. Grid synchronization of an inverter is the process of aligning the inverter's output with the grid's voltage, frequency, and phase, enabling the two systems to work together seamlessly [17]. Using sensors, the inverter continuously monitors the grid's parameters-voltage, frequency, and phase angle. It ensures that the grid remains within acceptable limits, such as voltage magnitude and frequency stability, for successful synchronization. A Phase-Locked Loop (PLL) is typically employed to synchronize the inverter's output phase and frequency with the grid [18]. The PLL dynamically adjusts the inverter's output to track the grid's phase angle accurately.

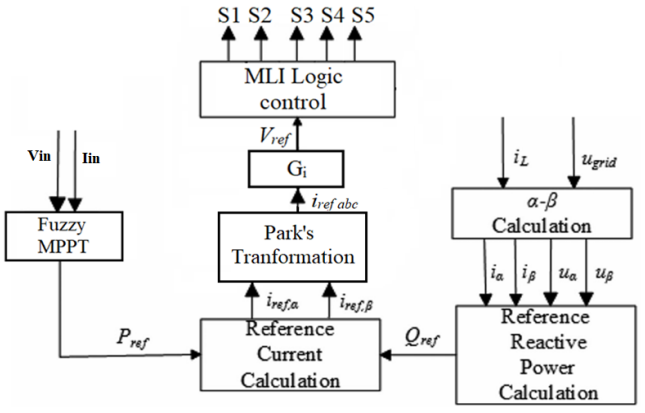

Fig. 5 Modified p-q control scheme for proposed MLI

During the synchronization process, the inverter gradually increases its output power to avoid sudden surges that could destabilize the grid. Once synchronized, the inverter injects current into the grid, typically operating at a power factor close to unity to minimize reactive power flow. In systems such as solar or wind, the fluctuating input power makes stable synchronization challenging. Proper grid synchronization ensures stability, efficiency, and compliance with grid codes. Inverter designs often incorporate advanced algorithms, robust hardware, and real-time monitoring to effectively manage dynamic grid conditions [19]. A robust synchronized controller module with reduced complexity should be introduced to implement these recommendations. The modified p-q control theory, including input and output signals, is illustrated in Figure 5. Figure 5 shows that the controller generates the reference signal with respect to the active power reference (P_{ref}) and reactive power references (Q_{ref}) signals. The P_{ref} *signal* is calculated by the Fuzzy MPPT technique, which has a faster response to the changes in the V_{pv} and I_{pv} signals [20]. The change in P_{ref} value with respect to the V_{pv} and I_{pv} signals is generated by the fuzzy-based MPPT technique, which uses two input variables and one output variable [21]. Each variable, V_{pv} and I_{pv} are set with seven membership functions fuzzified using 49 rule-base. On the other side, the Q_{ref} signal is calculated from the grid voltage (u_{grid}) and load current (i_L) [19]. The Q_{ref} signal is calculated from the αβ components of u_{grid} and i_L generated by Clark's transformation expressed as:

$$\begin{bmatrix} F\alpha \\ F\beta \end{bmatrix} = \frac{2}{3} * \begin{bmatrix} 1 & -\frac{1}{2} & -\frac{1}{2} \\ 0 & \frac{\sqrt{3}}{2} & -\frac{\sqrt{3}}{2} \end{bmatrix} \begin{bmatrix} Fa \\ Fb \\ Fc \end{bmatrix} \quad (3)$$

Here, F can be any signal, either voltage or current.

$$Q_{ref} = u_\beta i_\alpha - u_\alpha i_\beta \quad (4)$$

From the P_{ref} and Q_{ref} signals the αβ reference current signals ($i_{ref.\alpha}$ and $i_{ref.\beta}$) are generated as per the expressions below.

$$\begin{bmatrix} i_{\alpha,ref} \\ i_{\beta,ref} \end{bmatrix} = \frac{1}{u_{\alpha\beta}^2} \begin{bmatrix} u_\alpha & -u_\beta \\ u_\beta & u_\alpha \end{bmatrix} \begin{bmatrix} P_{ref} \\ Q_{ref} \end{bmatrix} \quad (5)$$

For the reference signals to control the MLI using the Logic Gate controller using inverse Clark's transformation is expressed as:

$$\begin{bmatrix} F_{a-ref} \\ F_{b-ref} \\ F_{c-ref} \end{bmatrix} = G_i \begin{bmatrix} 1 & 0 \\ -\frac{1}{2} & \frac{\sqrt{3}}{2} \\ -\frac{1}{2} & -\frac{\sqrt{3}}{2} \end{bmatrix} \begin{bmatrix} F_\alpha \\ F_\beta \end{bmatrix} \quad (6)$$

Here, G_i is the gain for per unit reference voltage conversion gain values given as per the response of the inverter. These reference signals (F_{a-ref}, F_{b-ref}, F_{c-ref}) are used for the generation of pulses for three phase MLI.

4. Simulation Analysis

All the blocks and modules of the proposed 'three-phase grid interconnection of PV array and wind farm with transformer-less boost multilevel inverter' topology are considered from the 'Electrical' subset of the Simulink library browser. The controller blocks are taken from 'Continuous' 'Signal Routing' and 'Commonly Used Blocks'. The measurements are plotted in graphical representation using 'Scope' blocks with time as reference. All system components are updated with the parameters given in Table 2.

Table 2. Configuration parameters

Name of the Element	Parameters
Grid	V_{grid} = 400V_{rms}, 50Hz, Lg = 8mH
PV array	Manufacturer: SunPower SPR-300NE-WHT-D V_{mp} = 54.7V, V_{oc} = 64V, I_{mp} = 5.49A, I_{sc} = 5.87A, N_s = 2, N_p = 15. P_{pv} = 9Kw
PMSG	P_{nom} = 4kW, R_s = 0.129Ω, L_s = 1.53mH, Φ = 0.1821V.s, J = 0.003334kg.m^2, F = 0.000425N.m.s, p = 4
Wind turbine	P_m= 4kW, Base wind speed = 12m/s, maximum power at base wind speed = 1pu, Base rotational speed = 1.2pu, Pirch angle = 0.05deg.
Inverter	C_{in} = 600μF, R_{igbt} = 1mΩ, L_f = 2.8mH, C_f = 5.5μF, P_{load} = 3kW
Control	MPPT gain = 0.1, Current gain = 1,

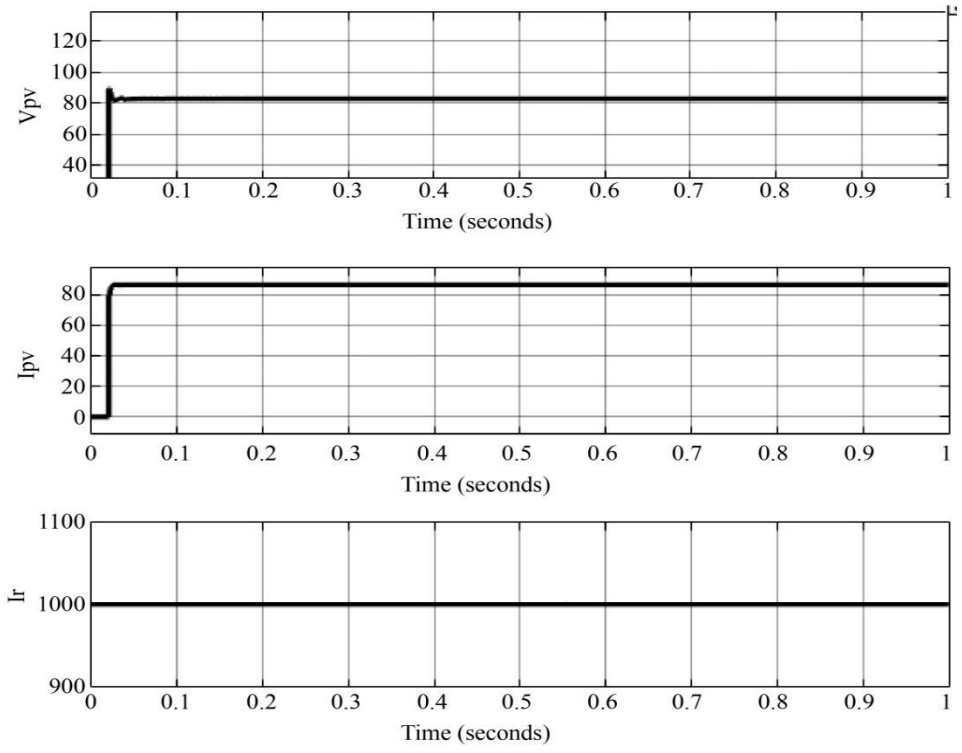

Fig. 6 PV array characteristics

Per the PV characteristics in Figure 6, the solar radiation is maintained stable at 1000W/m2 throughout the simulation of 1sec. The voltage of the PV array is recorded to be 83V, which is the Voltage at maximum power (Vmp). The current extracted from the PV array is 86A, producing a total power extraction of 7.1kW from the panels. The graph of power extracted from the PV array is presented in Figure 7.

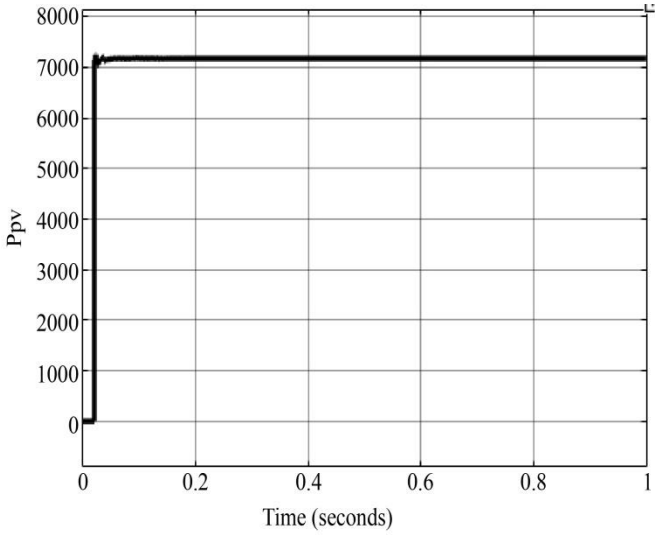

Fig. 7 PV array power

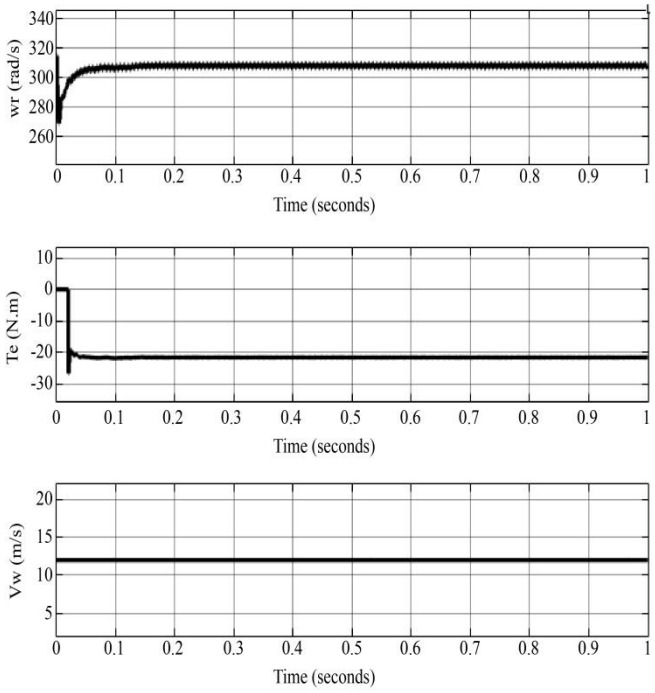

Fig. 8 Wind farm characteristics

Figure 8 represents the PMSG characteristics, showing the rotor speed, electromagnetic torque and wind speed. The total power extracted from the PMSG wind farm is 3.3kW, as presented in Figure 9.

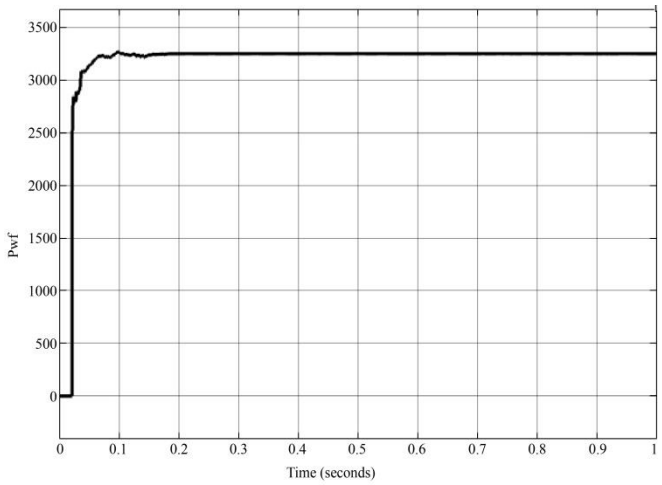

Fig. 9 PMSG wind farm injected power

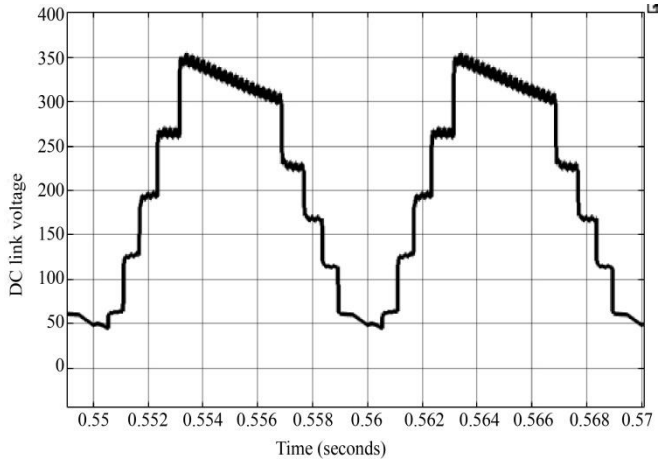

Fig. 10 Multi-level DC link voltage

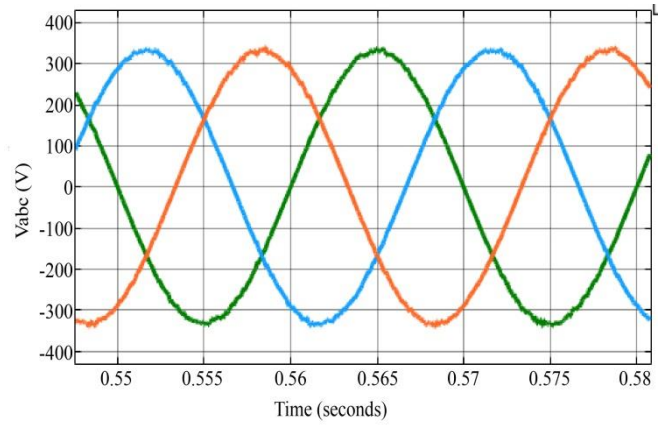

Fig. 11 PCC voltages

After the boosting of the PV array and wind farm voltages by the boost converter, the voltage levels created by the voltage level generator circuit are presented in Figure 10. As per Figure 10, the maximum voltage generated by the voltage level generator circuit is 325V, which is 4 times the input PV array voltage of 80V.

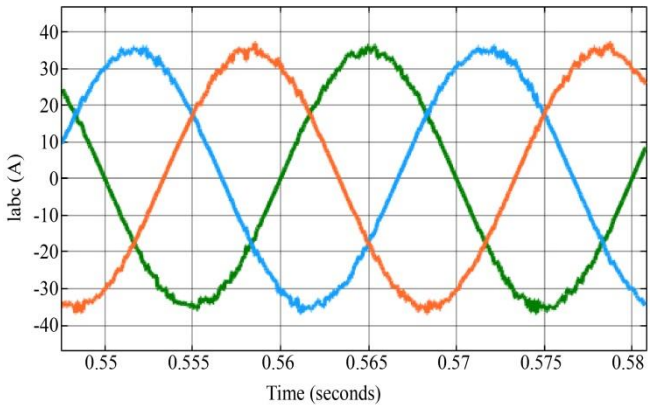

Fig. 12 Inverter current

The multilevel voltage is inverted by the switches Q1-Q4 as per the synchronization to the grid voltage. The voltage at the PCC of the system is measured and presented in Figure 11. For the same MLI with 11-level AC voltage generation, the inverter current injected into the load is presented in Figure 12. The PCC voltage has a maximum value generated at 325V, the maximum value of 230Vrms AC voltage. The maximum value is maintained constant throughout the simulation of 1sec. Figure 13 shows the active powers measured at the inverter output, grid, and load modules. For a total load demand of 10370W, the PV array compensates for 7184W, and the wing farm compensates for 3185W, sharing power with the load. As the complete power is mostly compensated by the PV array and wind farm, the grid power is recorded to be low at 156W.

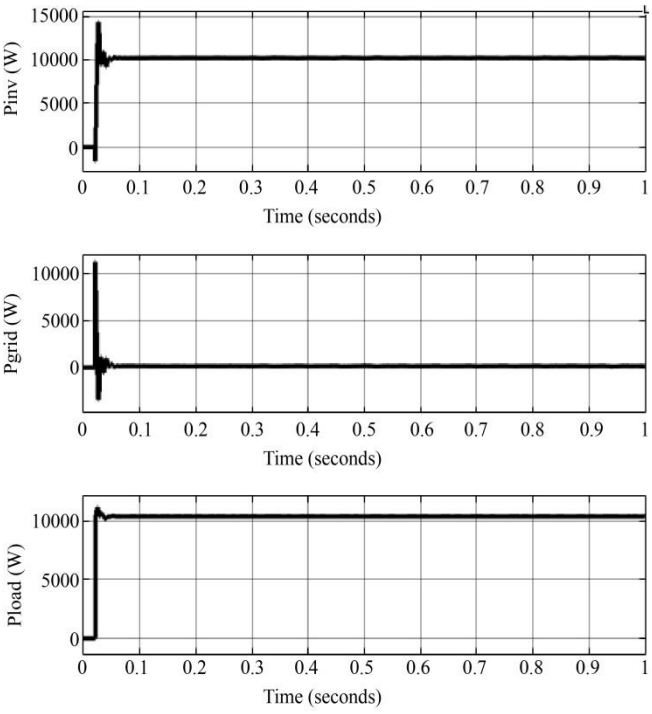

Fig. 13 Active powers of inverter, grid and load

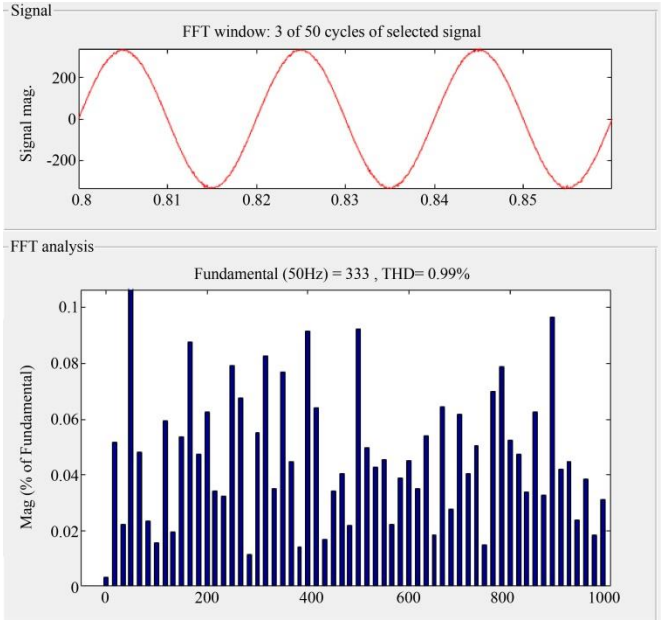

Fig. 14 PCC voltage THD

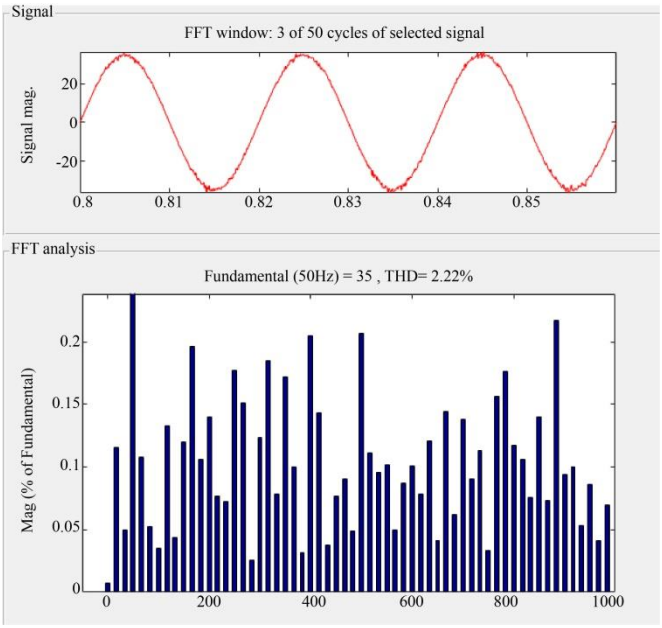

Fig. 15 Inverter current THD

Figures 14 and 15 presented are the THD values of the PCC voltage and inverter current calculated to be 0.99% and 2.22%. The THD values of the voltage and current are determined using the 'powergui' FFT analysis tool for a fundamental frequency of 50Hz.

5. Conclusion

Implementing a 'three-phase grid interconnection of PV array with transformer-less boost multilevel inverter' topology is achieved using MATLAB tools. The simulation is carried out with stable solar irradiation set in the model, extracting 7kW from the PV array and 3kW from the PMSG

wind farm in complete simulation time. The MLI creates a nine-level AC voltage using the switches S1-S5 and Q1-Q4 at the fundamental frequency of the grid. The power from the PV array is shared at the PCC compensating load with a power of 10kW. From the complete load demand of 10kW, the PV array compensates for 7kW, and the wind farm compensates for 3kW. With the MLI connected to the PV array, the THD of the PCC voltage is reduced to a very low value of 0.99%, which is in the permissible range of the IEEE 519-2022 standard. The power from the PV array is shared with the grid through the proposed boosting transformer-less MLI with a voltage gain of 4 and reduced harmonic content.

References

[1] Mikalai Filonchyk et al., "Greenhouse Gases Emissions and Global Climate Change: Examining the Influence of CO2, CH4, and N2O," *Science of The Total Environment*, vol. 935, 2024. [CrossRef] [Google Scholar] [Publisher Link]

[2] Kashif Abbass et al., "A Review of The Global Climate Change Impacts, Adaptation, and Sustainable Mitigation Measures," *Environmental Science and Pollution Research*, vol. 29, pp. 42539-42559, 2022. [CrossRef] [Google Scholar] [Publisher Link]

[3] Muhammad Kabir et al., "Climate Change Due to Increasing Concentration of Carbon Dioxide and Its Impacts on Environment in 21st Century; A Mini Review," *Journal of King Saud University-Science*, vol. 35, no. 5, pp. 1-7, 2023. [CrossRef] [Google Scholar] [Publisher Link]

[4] Abidur Rahman, Omar Farrok, and Md. Mejbaul Haque, "Environmental Impact of Renewable Energy Source Based Electrical Power Plants: Solar, Wind, Hydroelectric, Biomass, Geothermal, Tidal, Ocean, And Osmotic," *Renewable and Sustainable Energy Reviews*, vol. 161, 2022. [CrossRef] [Google Scholar] [Publisher Link]

[5] Abdalla Y. Mohammed, Farog I. Mohammed, and Mamoun Y. Ibrahim, "Grid-Connected Photovoltaic System," *2017 International Conference on Communication, Control, Computing and Electronics Engineering*, Khartoum, Sudan, pp. 1-5, 2027. [CrossRef] [Google Scholar] [Publisher Link]

[6] Marcolino Humberto Díaz-Araujo et al., "Analysis of Grid-Connected Photovoltaic Generation Systems in the Harmonic Domain," *Energies*, vol. 12, no. 24, pp. 1-14, 2019. [CrossRef] [Google Scholar] [Publisher Link]

[7] Sachin Jain, and Vivek Agarwal, "A Single-Stage Grid Connected Inverter Topology for Solar PV Systems with Maximum Power Point Tracking," *IEEE Transactions on Power Electronics*, vol. 22, no. 5, pp. 1928-1940, 2007. [CrossRef] [Google Scholar] [Publisher Link]

[8] Samuel Vasconcelos Araujo, Peter Zacharias, and Regine Mallwitz, "Highly Efficient Single-Phase Transformer-Less Inverters for Grid-Connected Photovoltaic Systems," *IEEE Transactions on Industrial Electronics*, vol. 57, no. 9, pp. 3118-3128, 2021. [CrossRef] [Google Scholar] [Publisher Link]

[9] Anurag Priyadarshi, Pratik Kumar Kar, and Srinivas Bhaskar Karanki, "A Single Source Transformer-Less Boost Multilevel Inverter Topology with Self-Voltage Balancing," *IEEE Transactions on Industry Applications*, vol. 56, no. 4, pp. 3954-3965, 2020. [CrossRef] [Google Scholar] [Publisher Link]

[10] Kasinath Jena et al., "Transformer-Less Multilevel Inverter (TMLI) with Reduced Device Count and Voltage Stress," *e-Prime-Advances in Electrical Engineering, Electronics and Energy*, vol. 7, pp. 1-11, 2024. [CrossRef] [Google Scholar] [Publisher Link]

[11] Mohamed Trabelsi, Hani Vahedi, and Haitham Abu-Rub, "Review on Single-DC-Source Multilevel Inverters: Topologies, Challenges, Industrial Applications, and Recommendations," *IEEE Open Journal of the Industrial Electronics Society*, vol. 2, pp. 112-127, 2021. [CrossRef] [Google Scholar] [Publisher Link]

[12] Mohammad Amani, Milad Niaz Azari, and Mohammad Rezanejad, "Single Source Self-Balanced Switched-Capacitor Multilevel Inverter with Reduced Number of Semiconductors," *IET Power Electronics*, vol. 16, no. 4, pp. 575-583, 2022. [CrossRef] [Google Scholar] [Publisher Link]

[13] Emad Samadaei et al., "Single DC Source Multilevel Inverter with Changeable Gains and Levels for Low-Power Loads," *Electronics*, vol. 9, no. 6, pp. 1-15, 2020. [CrossRef] [Google Scholar] [Publisher Link]

[14] Jiahui Jiang, Zhihao Liang, and Huicui Wang, "A Comprehensive Review on Single DC Source Multilevel Inverters for Renewable Energy Applications," *Electrical Engineering*, vol. 105, no. 6, pp. 3895-3917, 2023. [CrossRef] [Google Scholar] [Publisher Link]

[15] Akanksha Kumari et al., "A Single Source Five-Level Switched-Capacitor Based Multilevel Inverter with Reduced Device Count," *e-Prime-Advances in Electrical Engineering, Electronics and Energy*, vol. 5, pp. 1-14, 2023. [CrossRef] [Google Scholar] [Publisher Link]

[16] Mohamed Trabelsi, Hani Vahedi, and Haitham Abu-Rub, "Review on Single-Dc-Source Multilevel Inverters: Topologies, Challenges, Industrial Applications, and Recommendations," *IEEE Open Journal of the Industrial Electronics Society*, vol. 2, pp. 112-127, 2021. [CrossRef] [Google Scholar] [Publisher Link]

[17] Asim Datta, Rishiraj Sarker, and Imraj Hazarika, "An Efficient Technique Using Modified p-q Theory for Controlling Power Flow in a Single-Stage Single-Phase Grid-Connected PV System," *IEEE Transactions on Industrial Informatics*, vol. 15, no. 8, pp. 4635-4645, 2019. [CrossRef] [Google Scholar] [Publisher Link]

[18] Haoyan Liu, Yuzhi Zhang, and H. Alan Mantooth, "Residential Renewable Energy Distribution System with PQ Control," *2015 IEEE International Conference on Building Efficiency and Sustainable Technologies*, Singapore, pp. 33-38, 2015. [CrossRef] [Google Scholar] [Publisher Link]

[19] Min-Rong Chen et al., "Optimal P-Q Control of Grid-Connected Inverters in a Microgrid Based on Adaptive Population Extremal Optimization," *Energies*, vol. 11, no. 8, pp. 1-19, 2018. [CrossRef] [Google Scholar] [Publisher Link]

[20] Saban Ozdemir, Necmi Altin, and Ibrahim Sefa, "Fuzzy Logic Based MPPT Controller for High Conversion Ratio Quadratic Boost Converter," *International Journal of Hydrogen Energy*, vol. 42, no. 28, pp. 17748-17759, 2017. [CrossRef] [Google Scholar] [Publisher Link]

[21] B.G. Sujatha, and G.S. Anitha, "Enhancement of PQ in Grid Connected PV System Using Hybrid Technique," *Ain Shams Engineering Journal*, vol. 9, no. 4, pp. 869-881, 2018. [CrossRef] [Google Scholar] [Publisher Link]